J. Fluid Mech. (1970), *vol.* 40, *part* 4, *pp.* 737–751
Printed in Great Britain

Diurnal tides and shear instabilities in a rotating cylinder

By RORY THOMPSON
Department of Atmospheric Sciences, Oregon State University, Corvallis

(Received 21 April 1969 and in revised form 27 October 1969)

Any slight tilt or tide on the fluid in a rotating cylinder causes periodic motions, whose radiation pressures in the viscous boundary layers force mean differential rotations of the fluid, which are found numerically. At certain fluid depths, even very small tilts can cause shears large enough for perturbations to overcome Ekman friction, causing turbulence. An experiment confirms the theory.

1. Introduction

The most common geophysical fluid dynamic laboratory models involve annuli, including cylinders. Thus it is reasonable to study the models' responses to extraneous influences such as tides or imperfections of rotation, especially since one can hope to actually find solutions and compare them with experiments, unlike the real-world flows. Baines (1967) theoretically studied axisymmetric forced oscillations of a finite rotating cylinder and found that the asymptotic periodic flow contains pseudo-random patterns of internal shear for forcing slower than the rotation frequency. Aldridge (1967) experimentally studied axisymmetric modes of a rotating sphere excited by a small torsional oscillation. For rotating annuli, visible effects of the misalignment of the axis of rotation were noted by Fultz *et al.* (1959) and McDonald & Dicke (1967), but apparently the only previous studies of the effects have been by Fultz (1965) and Crow (1965). Fultz found that the water in a rotating, tilted rectangular box developed a powerful central vortex for a certain range of water depths. Crow found the same for a cylinder and showed that the depth of the water when a vortex occurred was near that of a resonance of inviscid fluid in a cylinder with an artificial pressure to keep the surface plane.

The radius is R, the viscosity is μ, and the mean depth of the water is H. The usual cylindrical co-ordinates are taken rotating with the cylinder, so z is along its axis, r is radial, and θ is counter-clockwise. The angular velocity Ω is chosen positive. So, the height around which to linearize is

$$H + (\Omega^2/2g)\,(r^2 - \tfrac{1}{2}R^2) + \epsilon r \cos(\theta + \Omega t),$$

choosing θ counter-clockwise from the projection of $\boldsymbol{\Omega}$ onto the horizontal. The deviation from this depth is denoted η. Let u be the radial velocity dr/dt, v be the tangential velocity $r\,d\theta/dt$, and w be the vertical velocity dz/dt. Let p be the deviation pressure from hydrostatic, which latter includes centrifugal force and

the (rotating) horizontal component of gravity as well as the vertical component. Surface tension is neglected. Now scale t by Ω^{-1}, r and z by R, u, v, and w by $\epsilon\Omega R$, p by $\epsilon R^2\Omega^2$, and η by ϵFR, where $F = \Omega^2 R/g$. Also define $E = \nu/\Omega H^2$.

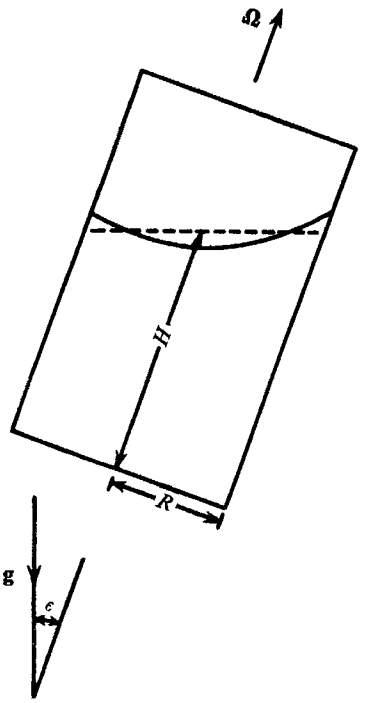

FIGURE 1. Schematic diagram, showing notation: the cylinder is rotating at angular velocity $\boldsymbol{\Omega}$ about its axis of symmetry at angle ϵ from vertical.

Expand the non-dimensional variables in the small parameter ϵ, so

$$u = u_0 + \epsilon u_1 + O(\epsilon^2),$$

etc. and separate the coefficients of ϵ to get the zero-order (linear) equations (1.1).

$$\left.\begin{aligned}
\frac{\partial u_0}{\partial t} &= -\frac{\partial p_0}{\partial r} + 2v_0 + E\left(\nabla^2 u_0 - \frac{u_0}{r^2} - \frac{2}{r^2}\frac{\partial v_0}{\partial \theta}\right)\frac{H^2}{R^2},\\
\frac{\partial v_0}{\partial t} &= -\frac{\partial p_0}{r\,\partial \theta} - 2u_0 + E\left(\nabla^2 v_0 - \frac{v_0}{r^2} + \frac{2}{r^2}\frac{\partial u_0}{\partial \theta}\right)\frac{H^2}{R^2},\\
\frac{\partial w_0}{\partial t} &= -\frac{\partial p_0}{\partial z} + E\nabla^2 w_0 \frac{H^2}{R^2},\\
\frac{\partial u_0}{\partial r} + \frac{u_0}{r} + \frac{\partial v_0}{r\,\partial \theta} + \frac{\partial w_0}{\partial z} &= 0.
\end{aligned}\right\} \tag{1.1}$$

The zero-order inviscid boundary conditions are

$$w_0 = 0 \quad \text{at} \quad z = 0,$$

$$u_0 = 0 \quad \text{at} \quad r = 1 \quad \text{and no singularity at} \quad r = 0,$$

and $$p_0 = \eta_0,$$

$$w_0 = -r\sin(\theta+t) + F(\partial\eta_0/\partial t) + Fu_0 r$$

at $$z = \tfrac{1}{4}F(2r^2-1) + H/R.$$

2. Zero-order interior solution

In the interior, E is negligible ($O(10^{-5})$ in the experiments discussed later), so set $E = 0$. The equations are linear, so, only keeping the driven components of flow, write

$$w_0 = w(r,z)\sin(\theta+t), \quad \eta_0 = \eta(r)\cos(\theta+t), \quad \text{etc.},$$

and combine the resultant equations to get

$$\frac{\partial^2 p}{\partial r^2} + \frac{1}{r}\frac{\partial p}{\partial r} - \frac{p}{r^2} = 3\frac{\partial^2 p}{\partial z^2}, \tag{2.1}$$

with boundary conditions

$$\frac{\partial p}{\partial z} = 0 \quad \text{at} \quad z = 0,$$

$$\frac{\partial p}{\partial r} + \frac{2p}{r} = 0 \quad \text{at} \quad r = 1,$$

$$\frac{\partial p}{\partial z} = r + \frac{Fp}{3} - \frac{Fr}{3}\frac{\partial p}{\partial r} \quad \text{at} \quad z = \tfrac{1}{4}F(2r^2-1) + H/R.$$

By the usual separation techniques, the solution is of the form,

$$p = \sum_{n=1}^{\infty} A_n \cos\left(\frac{\lambda_n z}{\sqrt{3}}\right) J_1(\lambda_n r), \tag{2.2}$$

with λ to solve $$\lambda J_1'(\lambda) + 2J_1(\lambda) = 0. \tag{2.3}$$

For $\lambda^2 < 0$, there is no non-zero $\mu = i\lambda$ which satisfies $\mu I_1'(\mu) + 2I_1(\mu) = 0$, since $I_1(x) = iJ_1(ix)$ is monotonic. Using the Bessel function tables of Abramowitz & Stegun (1965), the first five roots of (2.3) were found to be

$$\lambda_1 = 2{\cdot}735, \quad \lambda_2 = 5{\cdot}691, \quad \lambda_3 = 8{\cdot}767, \quad \lambda_4 = 11{\cdot}875 \quad \text{and} \quad \lambda_5 = 14{\cdot}997.$$

The motions corresponding to these eigenvalues are plainly inertial waves, which will be influenced by gravity through the surface boundary condition. Each of the modes satisfies the homogeneous bottom and side boundary conditions; a sum is necessary to satisfy the inhomogeneous surface boundary condition. Unfortunately, as well as being inhomogeneous, it is inseparable, so some sort of expansion is necessary. F is small in the experiments, so it can be used as the expansion parameter. Using a Taylor expansion in F, the surface condition is

$$\frac{\partial p}{\partial z} + \frac{F}{4}(2r^2-1)\frac{\partial^2 p}{\partial z^2} = r + \frac{Fp}{3} - \frac{1}{3}Fr\frac{\partial p}{\partial r} + O(F^2) \tag{2.4}$$

at $z = H/R$. Perhaps such an expansion is questionable for the higher modes

(those for which $nF \gtrsim 1$), but these will not be studied much, since they are more susceptible to friction.

To make

$$\sum_{n=1}^{\infty} A_n \left\{ -\frac{\lambda_n}{\sqrt{3}} \sin\left(\frac{\lambda_n H}{\sqrt{3}R}\right) J_1(\lambda_n r) - \frac{F\lambda_n^2}{12} \cos\left(\frac{\lambda_n H}{\sqrt{3}R}\right) (2r^2-1) J_1(\lambda_n r) \right.$$
$$\left. -\frac{F}{3} \cos\left(\frac{\lambda_n H}{\sqrt{3}R}\right) J_1(\lambda_n r) + \frac{F\lambda_n}{\sqrt{3}} \cos\left(\frac{\lambda_n H}{\sqrt{3}R}\right) r J_1'(\lambda_n r) \right\} = r, \quad (2.5)$$

multiply each side by $rJ_1(\lambda_n r)$ and integrate over (0, 1). The resulting linear system determines the response $\{A_n\}$ unless the determinant is zero, in which case there is a resonance.

In the resulting infinite linear system, all of the off-diagonal terms are $O(F)$, so one may solve to $O(F)$ by just setting them to zero, to yield estimates for the first few coefficients of

$$\left.\begin{aligned} A_1 &= -2{\cdot}35/(s_1 + 0{\cdot}292Fc_1), \\ A_2 &= 0{\cdot}90/(s_2 - 0{\cdot}071Fc_2), \\ A_3 &= 0{\cdot}49/(s_3 - 0{\cdot}29Fc_3), \end{aligned}\right\} \quad (2.6)$$

where $s_1 = \sin(\lambda_1 H/\sqrt{3}R)$, etc.

While the system formally has a dense set of singular depths, one does not expect to see the higher modes, both because the coefficients decrease rapidly with n, and because viscosity will damp them more. The first few resonant depths, from (2.6), are

$$\left.\begin{aligned} (H/R)_1 &= 1{\cdot}990 - 0{\cdot}185F, \\ (H/R)_2 &= 0{\cdot}956 + 0{\cdot}022F,\ 1{\cdot}912 + 0{\cdot}022F, \\ (H/R)_3 &= 0{\cdot}621 + 0{\cdot}057F,\ 1{\cdot}241 + 0{\cdot}057F,\ 1{\cdot}862 + 0{\cdot}057F, \text{ etc.} \end{aligned}\right\} \quad (2.7)$$

These resonance depths, including the $O(F)$ corrections, will be exploited in the instability bounds of § 5.

3. Zero-order boundary solutions

While using a very small value for E allows viscosity to be ignored throughout most of the fluid, the high order terms become important in a region of relative height $E^{\frac{1}{2}}$ from the bottom. Rescaling (1.1) by $\zeta = E^{-\frac{1}{2}}z$, and dropping terms $O(E^{\frac{1}{2}})$, the boundary equations are:

$$\left.\begin{aligned} \frac{\partial u_0}{\partial t} &= -\frac{\partial p_0}{\partial r} + \frac{\partial^2 u_0}{\partial \zeta^2} + 2v_0, \\ \frac{\partial v_0}{\partial t} &= -\frac{\partial p_0}{r\,\partial\theta} + \frac{\partial^2 v_0}{\partial \zeta^2} - 2u_0, \\ 0 &= -\frac{\partial p_0}{\partial \zeta}, \\ \frac{\partial u_0}{\partial r} + \frac{u_0}{r} + \frac{\partial v_0}{r\,\partial\theta} + \frac{\partial w_0}{\partial \zeta} &= 0, \end{aligned}\right\} \quad (3.1)$$

with $$u_0 = v_0 = w_0 = 0 \quad \text{at} \quad \zeta = 0,$$

and the solution merges with the interior. This problem might be called a time-dependent Ekman layer problem. In the same fashion as the steady Ekman problem, and writing $\partial/\partial t \to i$, one gets

$$\frac{\partial^4 u_0}{\partial \zeta^4} - 2i\frac{\partial^2 u_0}{\partial \zeta^2} + 3u_0 = -\frac{2}{r}\frac{\partial p_0}{\partial \theta} - i\frac{\partial p_0}{\partial r},$$

which has characteristic roots $\pm(1-i)/\sqrt{2}$ and $\pm(1+i)\sqrt{\frac{3}{2}}$. Boundedness as $\zeta \to \infty$ excludes the roots with positive real parts, so imposing $u_0 = v_0 = w_0 = 0$ at $\zeta = 0$, restoring the factor e^{it}, and taking real parts, one has in the bottom boundary:

$$\left.\begin{aligned}
u_0 &= \sum \frac{A_n \lambda_n}{6}\Big\{(3J_0(\lambda_n r) + J_2)\sin(\theta+t) \\
&\quad - 3J_0 e^{-\zeta/\sqrt{2}}\sin\left(\theta + t + \frac{\zeta}{\sqrt{2}}\right) - J_2 e^{-\sqrt{\frac{3}{2}}\zeta}\sin(\theta + t - \sqrt{\tfrac{3}{2}}\zeta)\Big\}, \\
v_0 &= \sum \frac{A_n \lambda_n}{6}\Big\{(3J_0 - J_2)\cos(\theta+t) \\
&\quad - 3J_0 e^{-\zeta/\sqrt{2}}\cos\left(\theta + t + \frac{\zeta}{\sqrt{2}}\right) + J_2 e^{-\sqrt{\frac{3}{2}}\zeta}\cos(\theta + t - \sqrt{\tfrac{3}{2}}\zeta)\Big\}, \\
w_0 &= \sum A_n \lambda_n^2 J_1(\lambda_n r)\Big\{\tfrac{1}{3}z\sin(\theta+t) \\
&\quad - \frac{E^{\frac{1}{2}}}{2\sqrt{2}} e^{-\zeta/\sqrt{2}}\left[\cos\left(\theta + t + \frac{\zeta}{\sqrt{2}}\right) + \sin\left(\theta + t + \frac{\zeta}{\sqrt{2}}\right)\right] \\
&\quad + \frac{E^{\frac{1}{2}}}{6\sqrt{6}} e^{-\sqrt{\frac{3}{2}}\zeta}[-\cos(\theta + t - \sqrt{\tfrac{3}{2}}\zeta) + \sin(\theta + t - \sqrt{\tfrac{3}{2}}\zeta)] \\
&\quad + E^{\frac{1}{2}}\left(\frac{1}{2\sqrt{2}} + \frac{1}{6\sqrt{6}}\right)\cos(\theta+t) + E^{\frac{1}{2}}\left(\frac{1}{2\sqrt{2}} - \frac{1}{6\sqrt{6}}\right)\sin(\theta+t)\Big\}.
\end{aligned}\right\} \tag{3.2}$$

Thus, the effective vertical velocity at the bottom of the interior is

$$W_0|_{z=0} = \sum A_n \lambda_n^2 J_1(\lambda_n r) E^{\frac{1}{2}}\left[\left(\frac{1}{2\sqrt{2}} + \frac{1}{6\sqrt{6}}\right)\cos(\theta+t) + \left(\frac{1}{2\sqrt{2}} - \frac{1}{6\sqrt{6}}\right)\sin(\theta+t)\right]; \tag{3.3}$$

this can be combined with the pressure at the bottom to find the net energy flux out of the bottom

$$\int_0^1 \int_0^{2\pi} w_0 p_0 r\, d\theta\, dr = E^{\frac{1}{2}}\tfrac{1}{4}\pi \sum_n A_n^2 \lambda_n^2 \left(\frac{1}{2\sqrt{2}} + \frac{1}{6\sqrt{6}}\right) J_1^2(\lambda_n)\left(1 + \frac{3}{\lambda_n^2}\right). \tag{3.4}$$

The full viscous zero-order equations are given as (1.1). Considering the side boundary layers, write $s = \delta^{-1}(r-1)$, and expand in δ. The continuity equation and $u = 0$ at $s = 0$ force rescaling u by δ also. The viscous terms do not enter the equations in δ until $\delta = E^{\frac{1}{2}}$, so the interior equations hold outside an $E^{\frac{1}{2}}$ layer, and there is no need to consider an $E^{\frac{1}{3}}$ or $E^{\frac{1}{4}}$ layer. When $\delta = E^{\frac{1}{2}}$, p_0 is independent of s, the v_0 and w_0 equations are simple diffusion equations, the continuity equation may be integrated to give u_0, and the net energy flux out of the sides near

an nth resonance depth is

$$\int_0^{H/R}\int_0^{2\pi} u_0 p_0 \, d\theta \, dz = \pi E^{\frac{1}{2}} \frac{H}{R} \frac{A_n^2 \lambda_n}{12\sqrt{2}} J_1(\lambda_n)\,[2\lambda_n J_1(\lambda_n) - 3J_0(\lambda_n) + J_2(\lambda_n)]. \quad (3.5)$$

There must be an energy source to feed these sinks, and this is gravitational torque working on a viscously rotated centre of mass, since the fluid depth is not axisymmetric. If the centre of mass is rotated 90°, the torque and energy input will be maximized. Near a resonance depth, we need only consider the resonant component in the full Bessel expansion for the depth, for which the maximum energy generation is

$$\int_0^1\int_0^{2\pi} [A_n J_1(\lambda_n r)\sin(\theta+t)]\,[r\sin(\theta+t)]\, r\, d\theta\, dr = A_n \pi \frac{J_2(\lambda_n)}{\lambda_n}. \quad (3.6)$$

Setting this bound on the energy source equal to the sum of the two energy sinks gives an upper bound on a resonant component A_n,

$$\left.\begin{aligned} A_1 &\leqslant E^{-\frac{1}{2}}(0{\cdot}148)/(0{\cdot}146 + 0{\cdot}188\, H/R), \\ A_2 &\leqslant E^{-\frac{1}{2}}(0{\cdot}0170)/(0{\cdot}087 + 0{\cdot}224\, H/R), \\ A_3 &\leqslant E^{-\frac{1}{2}}(0{\cdot}0044)/(0{\cdot}067 + 0{\cdot}275\, H/R). \end{aligned}\right\} \quad (3.7)$$

These same bounds can be found, less physically, by using

$$\iiint p\left(\frac{\partial^2 p}{\partial r^2} + \frac{1}{r}\frac{\partial p}{\partial r} - \frac{p}{r^2} - 3\frac{\partial^2 p}{\partial z^2}\right) r\, d\theta\, dr\, dz = 0,$$

and integrating by parts, with the boundary conditions for (2.1) modified to include the $O(E^{\frac{1}{2}})$ contributions from (3.4) and (3.5). During revision of this paper, it was found that Gans (1969) used this latter technique on a very similar problem.

4. First-order mean motion

The mean motion only will be considered, denoted by a superbar. Since θ and t only occur in the combination $(\theta+t)$, a time average is also a θ average, i.e. a steady state has been reached. Write

$$\left.\begin{aligned} \mathscr{G}(r,z) &= \overline{u_0 \frac{\partial u_0}{\partial r}} + \overline{\frac{v_0}{r}\frac{\partial u_0}{\partial \theta}} + \overline{w_0 \frac{\partial u_0}{\partial z}} - \overline{\frac{v_0^2}{r}}, \\ \mathscr{H}(r,z) &= \overline{u_0 \frac{\partial v_0}{\partial r}} + \overline{\frac{v_0}{r}\frac{\partial v_0}{\partial \theta}} + \overline{w_0 \frac{\partial v_0}{\partial z}} + \overline{\frac{u_0 v_0}{r}}, \\ \mathscr{M}(r,z) &= u_0 \frac{\partial w_0}{\partial r} + v_0 \frac{\partial w_0}{r\,\partial \theta} + w_0 \frac{\partial w_0}{\partial z}. \end{aligned}\right\} \quad (4.1)$$

These are known from (3.2), though cumbersome.

Standard boundary-layer theory suggests splitting the problem into interior and boundary layers. The interior equations are:

$$\mathscr{G}(r,z) = -\frac{\partial \overline{p}_1}{\partial r} + 2\overline{v}_1, \quad (4.2)$$

$$0 = -2\bar{u}_1, \tag{4.3}$$

$$\mathscr{M}(r,z) = -\frac{\partial \bar{p}_1}{\partial z}, \tag{4.4}$$

$$\frac{\partial \bar{u}_1}{\partial r} + \frac{\bar{u}_1}{r} + \frac{\partial \bar{w}_1}{\partial z} = 0, \tag{4.5}$$

with boundary conditions to match the boundary solutions. $\mathscr{H}$ vanishes in the interior, since u_0 and v_0 are there out of phase. Equations (4.3) and (4.5) imply $\bar{w}_1$ is independent of z, which, with the kinematic free surface condition $\bar{w}_1 = rF\bar{u}_1$, implies $\bar{w}_1 = 0$.

Eliminating p between (4.2) and (4.4) gives

$$\frac{\partial \bar{v}_1}{\partial z} = \frac{1}{2}\frac{\partial \mathscr{G}}{\partial z} - \frac{1}{2}\frac{\partial \mathscr{M}}{\partial r}, \tag{4.6}$$

but leaves $\bar{v}_1$ ambiguous by any axially symmetric geostrophic flow. Since we are interested precisely in such, this is inconvenient.

Since the nth resonance is such that $\sin(\lambda_n H/\sqrt{3}R) = 0$, $\cos^2(\lambda_n H/\sqrt{3}R) = 1$, and

$$\int_0^{H/R} \frac{\partial \mathscr{G}}{\partial z}\, dz = \int_0^{H/R} \frac{\partial \mathscr{M}}{\partial r}\, dz = 0.$$

Thus, the vertical average of $\bar{v}_1$ is $\bar{v}_1(0+, r)$ near a resonance depth. Greenspan (1969) claims this is true for all depths. The bottom boundary determines this value.

Physically, one looks for steady flows in the boundary driven by radiation pressure. Return flows in the upper parts of boundary are relatively free of friction and require values $\bar{v}_1$ by conservation of angular momentum. Thus the boundary-layer flow determines the vertical average of $\bar{v}_1$ in the interior, through determining what pressure gradients $\partial \bar{p}_1/\partial r$ may be allowed. Suppress writing r, and apply scaling of the usual boundary variety ($\zeta = E^{-\frac{1}{2}}z$) to get the mean first-order flow in the boundary:

$$\left.\begin{aligned}
\mathscr{G}(\zeta) &= 2\bar{v}_1 + \frac{\partial^2 \bar{u}_1}{\partial \zeta^2} - \frac{\partial \bar{p}_1}{\partial r}, \\
\mathscr{H}(\zeta) &= -2\bar{u}_1 + \frac{\partial^2 \bar{v}_1}{\partial \zeta^2}, \\
0 &= \frac{\partial \bar{p}_1}{\partial \zeta}, \\
\frac{\partial \bar{u}_1}{\partial r} + \frac{\bar{u}_1}{r} + \frac{\partial \bar{w}_1}{\partial \zeta} &= 0, \\
\bar{u}_1 = \bar{v}_1 = \bar{w}_1 &= 0 \quad \text{at} \quad \zeta = 0, \\
\bar{u}_1 \quad \text{and} \quad \bar{w}_1 &\to 0 \quad \text{as} \quad \zeta \to \infty.
\end{aligned}\right\} \tag{4.7}$$

The system (4.7) is a two-boundary-value problem on an infinite interval. Of numerical solution methods, 'shooting' is the most convenient for determining the values $\partial p_1/\partial r$ which allow solution. Reformulate the w boundary conditions

via the continuity equation:

$$0 = \int_0^\infty \frac{\partial \overline{w}_1}{\partial \zeta} d\zeta = \left(\frac{\partial}{\partial r} + \frac{1}{r}\right) \int_0^\infty \overline{u}_1 \, d\zeta,$$

so

$$\int_0^\infty \overline{u}_1 \, d\zeta = S/r.$$

I.e. no vertical flux out implies the total horizontal flux is constant. For a cylinder, this flux must be zero at $r = 0$, so the boundary equations are:

$$\left.\begin{aligned} \mathscr{G} + c &= \frac{\partial^2 \overline{u}_1}{\partial \zeta^2} + 2\overline{v}_1, \\ \mathscr{H} &= \frac{\partial^2 \overline{v}_1}{\partial \zeta^2} - 2\overline{u}_1, \\ \overline{u}_1(0) &= \overline{v}_1(0) = 0, \\ \frac{\partial \overline{u}_1}{\partial \zeta} \quad &\text{and} \quad \frac{\partial \overline{v}_1}{\partial \zeta} \to 0 \quad \text{as} \quad \zeta \to \infty, \\ \int_0^\infty \overline{u}_1 \, d\zeta &= 0, \end{aligned}\right\} \tag{4.8}$$

where $\partial \overline{p}_1/\partial r$ is written c to emphasize its independence of ζ, and is determined by the five boundary conditions on the fourth-order equation.

One may note that there are no r derivatives in (4.8), so no boundary conditions in r may be satisfied, except by boundary layers. A discontinuity in v at $r = 0$ or at $r = 1$ will smooth out over a distance of $O(E^{\frac{1}{4}})$; see Stewartson (1957). At $r = 1$, one might worry about the zero-order forcing in the $E^{\frac{1}{2}}$ side-wall layers giving forced mean velocities $(\overline{u}, \overline{v}, \overline{w})$, but these can be taken as the inner boundary for an $E^{\frac{1}{3}}$ layer which will balance out $\overline{u}$ and $\overline{w}$. Then an $E^{\frac{1}{4}}$ layer will allow $\overline{v}$ to match the interior. Howard (1968) seems to be the first to have worked out the details for a general steady side-wall problem.

The system (4.8) can be numerically solved by simultaneously computing three independent solutions which all satisfy the conditions $\overline{u}_1 = \overline{v}_1 = 0$ at $\zeta = 0$. The outer boundary condition can be satisfied if there is a linear combination of the three solution vectors which satisfies $\partial u_1/\partial \zeta = \partial v_1/\partial \zeta = w_1 = 0$ as $\zeta \to \infty$, which is so if the determinant of these three variables for each of the three vectors goes to zero. If it does not, use the sign of the determinant to search for a better value for c, by bisecting the interval within which the zero is known to lie. Given c, $\overline{v}_1$ at the outer edge of the boundary layer is $\frac{1}{2}(\mathscr{G} + c)$, and is plotted for the first three resonances in figure 2. Note that a first-order vortex occurs at the origin in each case; one expects the discontinuity to smooth out through an $E^{\frac{1}{4}}$ boundary core. The exponentially growing possible solutions to the equations limited the integration to $\zeta \leqslant 12$. Fortunately, $\mathscr{G}$ and $\mathscr{H}$ had effectively reached their asymptotic values well before then, so the limitation was not serious.

Using the determinant approach avoided having to find the actual initial conditions necessary to hit the boundary conditions at infinity. This was highly necessary while shooting, for the undesired exponentially growing solutions rendered the solution highly unstable, as numerical experiments confirmed.

Thus, another technique is necessary to find the actual velocities in the boundary layer. Now that the eigenvalues $c(r, \lambda_n)$ are known, relaxation may be used. Liepmann relaxation in alternating directions was used, with a visual display to check for satisfactory convergence. With random initial conditions, the convergence was slow due to what appeared to be a close analogue to slowly decaying geostrophic oscillations, with sweep number in the place of time. Over-relaxation just increased the frequency. So, a small amount of damping (slight increase in the magnitude of the middle coefficient in the differencing scheme) was introduced and then relaxed to zero itself; thus very effectively damping the oscillations.

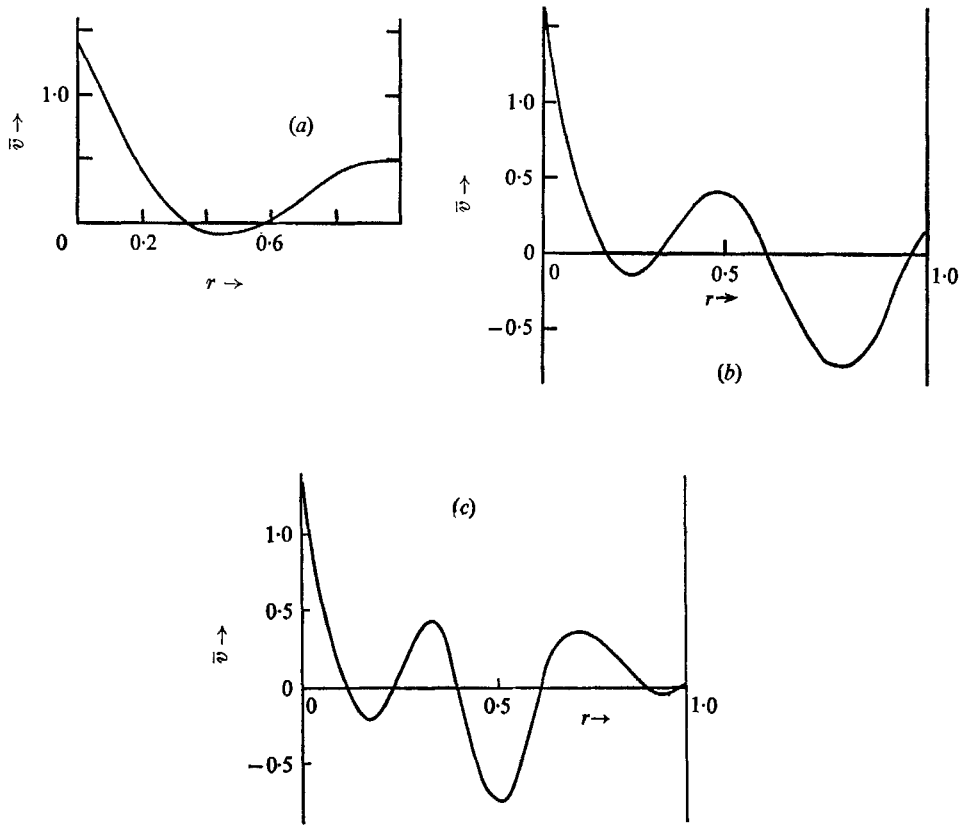

FIGURE 2. Non-dimensional mean azimuthal velocity at the top of the viscous boundary layer, for (*a*) the first resonance, (*b*) the second resonance, and (*c*) the third resonance.

The resultant non-dimensional radial mass fluxes in the boundary are sketched in figure 3 for the first three resonances. Features of interest about the depicted mass flux in the boundary layer are (i) that they represent somewhat distorted Ekman spirals and (ii) that the (closed) flows occur in n gyres for the nth resonance. These gyres, or ring vortices, will result in sweeping anything on the bottom into rings.

5. Possible shear instability

The last section showed that there will be mean tangential velocities $\bar{v}_1$ in the interior, and consequently shears. Thus there is a possibility of shear instabilities, for which we need to consider deviations of the first-order flow from the forced mean found in the last section. The deviation equations are

$$\frac{\partial \mathbf{u}_1}{\partial t} + (\mathbf{u}_0 . \nabla \mathbf{u}_0 - \overline{\mathbf{u}_0 . \nabla \mathbf{u}_0}) + 2\boldsymbol{\Omega} \times (\mathbf{u}_1 - \bar{\mathbf{u}}_1) = -\nabla(p_1 - \bar{p}_1). \tag{5.1}$$

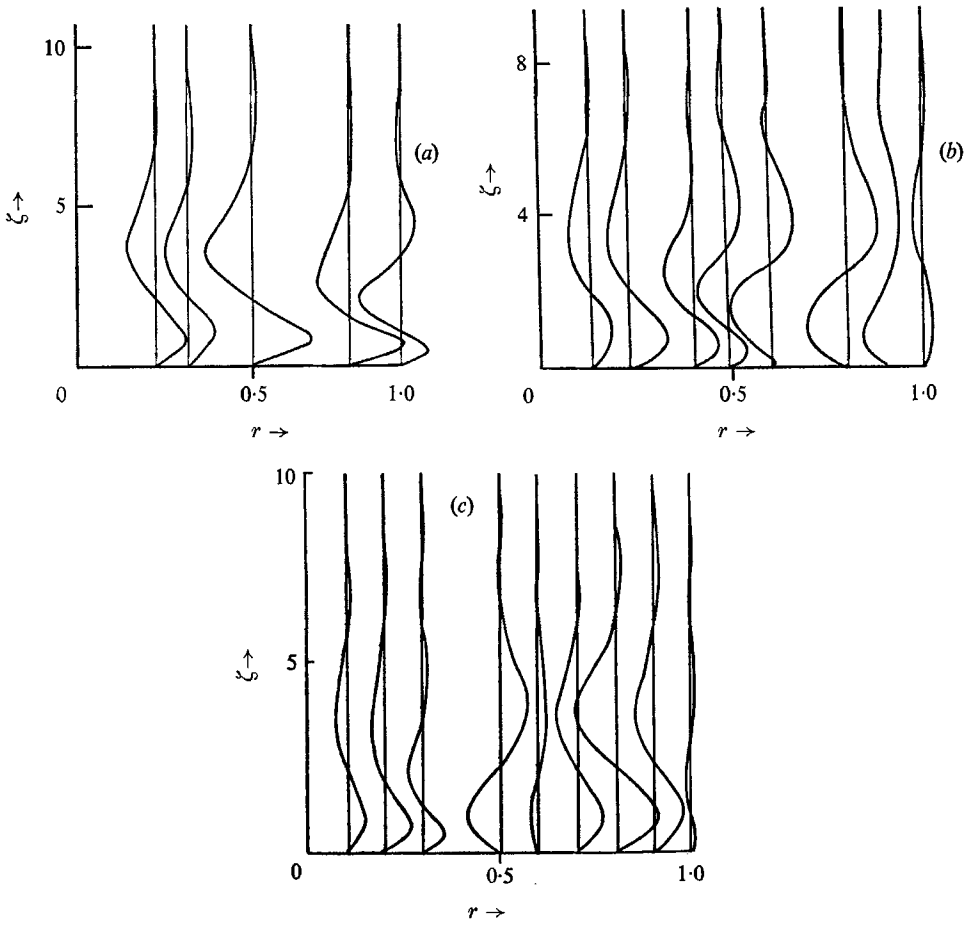

FIGURE 3. Non-dimensional radial mass flux in the viscous boundary layer, for (*a*) the first resonance, (*b*) the second resonance, and (*c*) the third resonance.

The friction terms may be neglected in the interior. The non-linear forcing from zero-order terms in (5.1) is purely periodic with twice the frequency of rotation of the cylinder, so if one averages (5.1) over one period, but not over θ, one has

$$\frac{\partial \tilde{\mathbf{u}}_1}{\partial t} + 2\boldsymbol{\Omega} \times (\tilde{\mathbf{u}}_1 - \bar{\mathbf{u}}_1) = -\nabla(\tilde{p}_1 - \bar{p}_1). \tag{5.2}$$

If the perturbations are slowly changing, as when near marginal instability, the first term will be small compared to the others. Then, taking the curl of (5.2),

$$(2\boldsymbol{\Omega}.\nabla)(\tilde{\mathbf{u}}_1-\bar{\mathbf{u}}_1)=0, \tag{5.3}$$

which says that slow deviations $(\tilde{\mathbf{u}}_1-\bar{\mathbf{u}}_1)$ follow the Taylor–Proudman theorem in being independent of z, even if the mean flow $\bar{\mathbf{u}}_1$ itself is not. Thus, it is reasonable to average $\bar{v}_1$ with respect to z and consider the motion as two-dimensional ..., especially since the instabilities were experimentally observed to be remarkably independent of z before this argument was thought of.

A scaling argument shows that, for such a system, the Ekman friction easily dominates lateral friction, so the latter will be neglected. This gives a barotropic shear problem which seems more relevant to geophysical fluid dynamics than the classical shear problems. Busse (1968) studies that problem in some generality. Since the effect of the surface slope turned out to be small, and complicating, the appropriate 'Rayleigh' stability equation is given by Busse's equation (3.3), which here becomes

$$(f-c)\left(\frac{d^2\chi}{dr^2}+\frac{1}{r}\frac{d\chi}{dr}-\frac{m^2\chi}{r}\right)-\left(\frac{3}{r}\frac{df}{dr}+\frac{d^2f}{dr^2}\right)\chi=0, \tag{5.4}$$

where the $\bar{v}_1$ scale is $E^{\frac{1}{2}}\Omega R$, $f=\bar{v}_1(rE^{\frac{1}{2}}\Omega R)^{-1}$, the perturbation pressure is $\chi(r)\exp\{i(m\theta-\epsilon\omega t)\}$, and the eigenvalue

$$c=\frac{\omega+i}{m}.$$

The interest centres on the resonances, when the instability occurs far enough away from the centre and f looks enough like a sinusoid to suggest that decent rough approximations for the eigenvalues c can be found from a Cartesian analogue with $V=V_0\cos kx$.

Then (5.4) becomes

$$(V-c)\left(\frac{d^2\psi}{dx^2}-m^2\psi\right)-\frac{d^2V}{dx^2}\psi=0. \tag{5.5}$$

Since c is complex, (5.5) is non-singular. Since the eigenvalue c is proportional to V_0, for large enough V_0 $\mathrm{Im}\,(c)$ will exceed $1/m$, so $\mathrm{Im}\,(\omega)>0$ and there will be instability. By symmetry of (5.5), $\mathrm{Re}\,(c)=0$, so the most unstable disturbance is sinuous, and Howard's (1961) semi-circle theorem and Høiland's (see Howard 1961) growth bound extend to give

$$|\mathrm{Im}\,(c)|=\left|\frac{\mathrm{Im}\,(\omega)+1}{m}\right|\leqslant V_0,$$

$$|\mathrm{Im}\,(\omega)+1|\leqslant \tfrac{1}{2}kV_0,$$

which imply necessary conditions for instability of

$$V_0>1/m,\quad V_0>2/k. \tag{5.6}$$

To get an improved estimate of c in (5.5), one may try a Galerkin method of approximating ψ by $\psi_0+\psi_1\exp(ikx)+\psi_{-1}\exp(-ikx)$, and making the error in

satisfying (5.5) orthogonal to the expansion functions. The resultant three homogeneous equations in ψ_0, ψ_1 and ψ_{-1} give factors zero and

$$c = \pm iV_0\left(\frac{k^2-m^2}{2(k^2+m^2)}\right)^{\frac{1}{2}},$$

which gives the minimum critical velocity as

$$V_0 = 3{\cdot}41/k \tag{5.7}$$

for $m = 0{\cdot}643k$. One expects a similar velocity shear somewhere to cause instability for the cylindrical case. Here, the velocity was scaled by $E^{\frac{1}{2}}\Omega R$, whereas $\bar{v}_1$ is scaled by $\epsilon^2\Omega R$. Thus (5.7) translates to

$$A_n^2\epsilon^2\,|V_0|\;\Omega R = 3{\cdot}41E^{\frac{1}{2}}(\Omega R/m_n^* R),$$

or

$$\epsilon = \left(\frac{3{\cdot}41}{|V_0|\;m_n^* R}\right)^{\frac{1}{2}}\frac{E^{\frac{1}{4}}}{A_n}, \tag{5.8}$$

where m_n^*, the dimensional wave-number for the nth resonance, is about $2\pi/(R/n)$, since about n rolls fit in one radius. From figure 2, a mean-square amplitude may be taken of $|V_0| \approx 0{\cdot}33$, $0{\cdot}41$ and $0{\cdot}31$ for the first three resonances.

The values of A_n are found from (2.7), for $F = 0{\cdot}145$, by trigonometric addition formulas, to be

$$\left.\begin{aligned} A_1 &= 2{\cdot}34\,|\sin(1{\cdot}65H/R)|^{-1},\\ A_2 &= 0{\cdot}90\,|\sin(3{\cdot}25H/R)|^{-1},\\ A_3 &= 0{\cdot}49\,|\sin(4{\cdot}7H/R)|^{-1}. \end{aligned}\right\} \tag{5.9}$$

Using $E^{\frac{1}{2}} = 1{\cdot}5 * 10^{-5}R/H$ to match the experiment, (5.8) and (5.9) give the approximate instability bounds

$$\left.\begin{aligned} \epsilon_1 &= 0{\cdot}034\,|\sin(1{\cdot}65H/R)|\;(R/H)^{\frac{1}{2}},\\ \epsilon_2 &= 0{\cdot}095\,|\sin(3{\cdot}25H/R)|\;(R/H)^{\frac{1}{2}},\\ \epsilon_3 &= 0{\cdot}20\,|\sin(4{\cdot}7H/R)|\;(R/H)^{\frac{1}{2}}, \end{aligned}\right\} \tag{5.10}$$

except for values of the sines small enough to cause the A_n's of (5.9) to be near the limits imposed by viscosity from (3.7). For instance, the smallest ϵ for $n = 1$ is

$$\left(\frac{3{\cdot}41}{(0{\cdot}44)\,(6{\cdot}28)}\right)^{\frac{1}{2}}\frac{E^{\frac{1}{4}}(0{\cdot}146+0{\cdot}188*1{\cdot}98)}{(0{\cdot}148)\,E^{-\frac{1}{2}}} \approx 3{\cdot}3\times10^{-4}.$$

From the smallest values of ϵ and (5.10), the instability bounds were plotted on figure 4. Where the tilt is large enough that the assumption of one resonant component being dominant seems doubtful, the bounds are dashed.

6. Experimental verification

It is time to show that the theory developed so far has some relation to reality. The turntable used was the 1 m table in the Fluid Dynamics Laboratory of the Woods Hole Oceanographic Institution, described in Ibbetson & Frazel (1965). Tilting was accomplished by a hand winch from a guard-rail to the 153 cm square steel plate upon which the turntable stood, allowing reasonably accurate

measurement of small angles. The cylinders used were clear plexiglass of radius 14·5 cm. A flat clear plastic sheet was used as a lid to get rid of torque from the air.

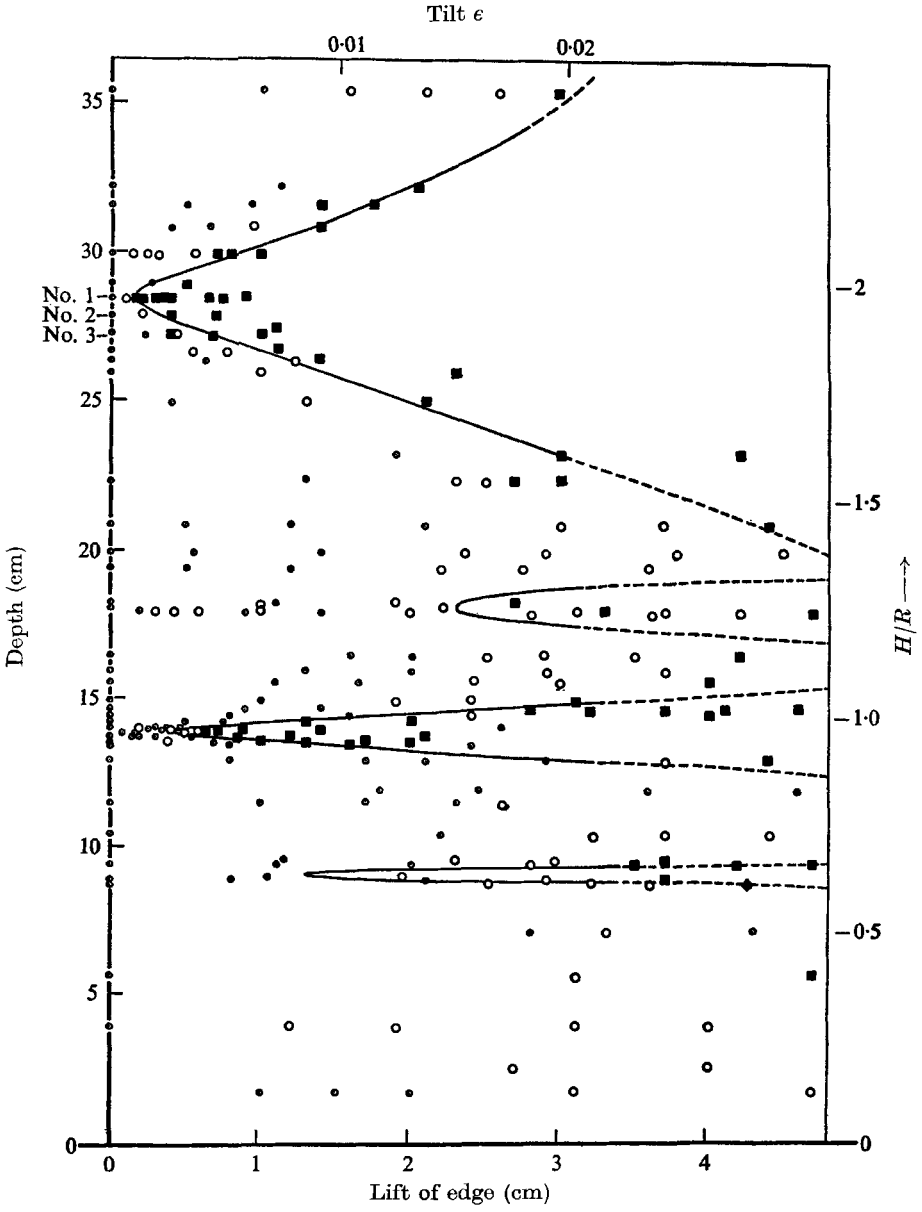

FIGURE 4. Experimental results and theoretical bounds, as explained in the text. ⊙, null; ○, rings; ■, unstable rings.

A typical run consisted of filling the cylinder to the desired depth with water mixed to room temperature, centring it on the turntable as closely as feasible, then speeding the turntable to 30 rpm, as determined with a stop watch. The fluid was allowed to spin up for at least twenty minutes, then potassium permanganate crystals were dropped through small holes in the lid. When spin-up

was complete, the turntable was carefully tilted and left, still spinning, for half an hour or more before tilting further. The results are plotted in figure 4. If nothing much was observed, a circled dot was entered. If rings of ink were observed, a large circle was entered. It may be worth noting that these rings were not due to the location of the dye crystals, for they normally sharpened up long after the crystals had dissolved and occasionally clear areas formed over a crystal, except for its thin plume going either in or out. At higher tilts, the rings became unstable to wavy disturbances, with large wave-numbers (30 and up) for outer rings and small wave-numbers (2 to 4) for inner rings. The instability observations are entered as heavy squares. Near resonances, the instability was violent enough that visible rings did not have time to form before powerful vortices formed. These vortices are presumably what Fultz and Crow observed, since they form most strongly near the first resonance. It may be worth noting that these vortices are not necessarily the first-order discontinuity vortex at the origin derived upon finding the theoretical $\bar{v}_1$ (though their continued existence may depend on similar causes), because they form from the instability on the inner ring when this grows slowly enough to be observed in detail.

Looking at the completed diagram, we see there is good agreement with the theory: there are resonances which get weaker as n increases, there are rings of convergence and divergence in the bottom boundary, and the predicted instability boundaries are near the experimental ones.

7. Conclusions

The tilted experiment discussed above is more suitable for checking the Ekman damping effects on barotropic shear instabilities than the experiment with which Busse (1968) compared his theory. The horizontal scale of the shears in that experiment were small enough that the internal dissipation was comparable to the Ekman dissipation; and, in fact, the theory and experiment disagreed by a factor of 2. Here the match is better, which suggests that the boundary-layer theory cannot only simplify the shear theory, but can also be useful in finding the responses of the fluid in the tilted cylinder. For certain geometries, having the axis of rotation precisely vertical can be important for geophysical laboratory models.

This paper formed a part of a thesis submitted to the Meteorology Department of the Massachusetts Institute of Technology. The author is indebted to Claes Rooth for suggesting the problem, Friedrich Busse for a helpful discussion, and L. N. Howard for being the thesis advisor. The Electrical Engineering Department of M.I.T. gave time on its PDP-1 computer, with which W. B. Ackermann helped. The paper is Contribution no. 2316 from the Woods Hole Oceanographic Institution (where it was completed). The author has been successively supported by the National Science Foundation, the Fannie and John Hertz Foundation, and the Office of Naval Research under contract N00014-66-CO241.

REFERENCES

ALDRIDGE, K. D. 1967 An experimental study of axisymmetric inertial oscillations of a rotating liquid sphere. Ph.D. Thesis, Massachusetts Institute of Technology.

ABRAMOWITZ, M. & STEGUN, T. A. 1965 *Handbook of Mathematical Functions.* Washington, D.C.: National Bureau of Standards.

BAINES, P. G. 1967 Forced oscillations of an enclosed rotating fluid. *J. Fluid Mech.* **30**, 533–46.

BUSSE, F. H. 1968 Shear flow instabilities in rotating systems. *J. Fluid. Mech.* **33**, 577–89.

CROW, S. 1965 Geophysical fluid dynamics participants lectures. Woods Hole Oceanographic Institution 21.

FULTZ, D. 1965 Talk at midwestern mechanics conference.

FULTZ, D., LONG, R. R., OWENS, G. V., BOHAN, W., KAYLOR, R. & WEIL, J. 1959 *Studies of Thermal Convection in a Rotating Cylinder with some Implications for Large-Scale Atmospheric Motions.* Boston, Mass.: Amer. Meteor. Soc.

GANS, R. 1969 On the precession of a resonant cylinder. *J. Fluid Mech.* (submitted).

GREENSPAN, H. P. 1969 On the non-linear interaction of inertial modes. *J. Fluid Mech.* **36**, 257–64.

HOWARD, L. N. 1961 A note on a paper by John W. Miles. *J. Fluid Mech.* **10**, 509–12.

HOWARD, L. N. 1968 Geophysical fluid dynamics lecture notes. Woods Hole Oceanographic Institution.

IBBETSON, A. & FRAZEL, R. E. 1965 The construction of a one metre diameter rotating table. W.H.O.I. ref. no. 65–41.

MCDONALD, B. E. & DICKE, R. H. 1967 Solar oblateness and fluid spin-down. *Science*, **158**, 1562-4.

STEWARTSON, K. 1957 On rotating laminar boundary layers. *Freiburg Symposium Boundary Layer Research*, pp. 59–71.